Desalination and Water Treatment
www.deswater.com
doi: 10.5004/dwt.2023.29516

293 (2023) 1–13
May

A novel dual-heated water and power cogeneration system using solar driven humidification–dehumidification cycle

Weifeng He[a,*], Qile Shi[a], Zihui Zhang[a], Zhaohui Yao[a], Pengfei Su[b,*], Dong Han[a]

[a]*Advanced Energy Conservation Research Group (AECRG), College of Energy and Power Engineering, Nanjing University of Aeronautics and Astronautics, Nanjing, China, Tel./Fax: +8602584893666; emails: wfhe@nuaa.edu.cn (W.F. He), shiqile@nuaa.edu.cn (Q. Shi), zhangzihui@nuaa.edu.cn (Z.H. Zhang), yaozhh@nuaa.edu.cn (Z.H. Yao), handong@nuaa.edu.cn (D. Han)*
[b]*Dongfang Turbine Co., Ltd., Deyang, China, Tel./Fax: +8602584893666; email: supengfei@dongfang.com (P.F. Su)*

Received 21 October 2022; Accepted 5 April 2023

ABSTRACT

A novel dual-heated water and power cogeneration system (WPCS), in which photovoltaic/thermal (PV/T) is used for seawater heating and electricity generation, and solar collector is applied for air heating, based on the humidification–dehumidification (HDH) cycle, is proposed. Comprehensive performance of the dual-heated WPCS is obtained, and the parametric analysis, from the pinch enthalpy difference (PED) within the humidifier and solar intensity, are accomplished. It is found the peak gained-output-ratio (GOR), water production and water production cost (WPC) 2.55, 76.32 kg·h^{-1} and 15.14 \$t^{-1}, with an uneconomical payback period (PBP). The parametric analysis implies a lower PED and higher solar intensity are profitable to raise the water production, while the GOR will decrease instead when the solar intensity rises. Furthermore, it is illustrated a higher PED and solar intensity can reduce the PBP. It is concluded the combined applications of the PV/T and solar collector can result in the advantages, to neutralize the features of the single heated, water- or air-heated HDH systems, HDH desalination methods for raising water production and GOR. However, the impossibility to recover the cost of the dual-heated WPCS within the working lifetime is also discovered, although this is of less importance in areas with water shortages.

Keywords: Dual-heated water and power cogeneration system; Photovoltaic/thermal; Humidification–dehumidification; Pinch enthalpy difference; Solar intensity

1. Introduction

Desalination, extensively applied to produce potable water, has drawn more and more attentions to relieve the water crisis for the arid areas. Thermal desalination stations coupled in the power plants, containing flashing [1], distillation [2] and thermal or mechanical vapor compression [3], were efficient satisfying the large-scale water demand, about 100–500,000 ton/d [4].

However, in the face of the small-scale fresh water demand, the energy conversion efficiency and economic performance will be limited due to the inherent features. A high efficient desalination method, called humidification and dehumidification type, which simulates the natural water cycle, was proposed, and the relevant advantages of energy conservation and compact structure [5–8] were validated in the past few years.

1.1. Literature review

Narayan [9] modelled various types of HDH desalination systems, in which the general effectiveness for the HDH processes was used. In addition, the fundamental discussion, innovative HDH cycles, such as the frames of thermal vapor compression [9], varied-pressure [10] and multi-extraction and injection [11,12], were advised to

* Corresponding authors.

update the conventional HDH desalination thermal cycle. It was proved the top GOR arrived at 1.22 at ideal conditions, verifying the potentials of the HDH desalination pattern.

In general, solar energy were always coupled with the HDH desalination systems [13] to heat the stream of seawater [14] or humid air [15]. Hamed [16] constructed the mathematical models of a solar based water-heated HDH desalination cycle, with the thermodynamic investigation completed. Two assigned periods, with 9 am to 17 pm and 13 pm to 17 pm, were arranged to investigate the water producing process, and a highest value was found during the later period because of different solar intensity. Besides the theoretical analysis, actual experimental test was also achieved to check the specific performance during heat and mass transferring, with the theoretical models validated. Saldivia [17] achieved a comprehensive analysis through experiments and numerical simulation for a solar based HDH desalination system, with an open-water, closed-air frame, and the numerical model was validated by the relevant test results. A new definition, the ratio of distillate and irradiance, was proposed to measure the desalination performance. An open-water and closed-air HDH frame, with a new direct absorption solar humidifier, was proposed by Dave [18], and influences of air flow rates and seawater flow rates on desalination performance were studied to clarify the operating status of solar humidifier. Comparison between the performance of the new and conventional system presented a promotion amplitude of 18.4% as for solar thermal energy efficiency, and the desalination cost was estimated within the scope of 0.007 to 0.035 $USDL^{-1}$. A non-dimensional thermodynamic investigation for a small-scale HDH desalination configuration, in which seawater was heated in the PV/T unit, was achieved by Simonetti [19]. Mathematical models to determine the optimal condition in a general formulation were proposed, based on the defined energy effectiveness, mass flow rate ratio of the seawater and air (MFRR) and water recovering ration from the feed seawater.

For another type of air-heated frame, Al-Sulaiman [20] used the parabolic trough solar collector for air heating in the HDH configuration, and the corresponding performance was focused, mainly referring to the impacts resulting from the layout of the solar collector. It was found the parabolic trough collector was appropriate for the air-heated pattern at the regions with high solar intensity. It was verified the air heater should be placed between the dehumidifier and humidifier for a high water producing efficiency. Extraction and injection were introduced into the air-heated HDH cycle by Negharchi [21], with the numerical results validated by the thermodynamic study. Regarding the actual prospects, the top water yield with a fixed collector, and the lowest energy expenditure with a fixed water yield, were obtained. It was seen the applied injection and extraction were helpful to optimize the performance, and there was a best injection and extraction rate in the HDH desalination thermal cycle. Besides, the exergy analysis for the devices was helpful to determine the optimal parameters. The HDH desalination configuration using the removed heat from the PV/T, with water production and PV cell power generation efficiency raised, was focused and studied by Giwa [22]. The practicability of an air-cooled HDH desalination system, driven by PV/T, and the relevant environmental friendliness in Abu Dhabi, were verified. It was discovered removing the thermal energy made a daily water yield of 2.28 L/m^2 of the PV cell. A declination amplitude of 83.6% under the environmental influences for the advised HDH desalination system was also found, in comparison with the PV and reverse osmosis configuration.

The previous literature involved with solar energy mainly focused on the single heated HDH desalination patterns, and the related performance, especially the thermodynamic aspect, were extensively investigated. Actually, the dual-heated HDH desalination system was also proposed by Yildirim [23], and the performance was theoretically studied for different conditions in Antalya, Turkey. Theoretical models were developed according to the Runge–Kutta method. Yields in 1 d and year of the desalination system were calculated for three operation modes, including air heating, water heating and combined heating. After the performance simulation, it was found that the combined mode had a higher daily water production compared to the single heating modes. In terms of water/power cogeneration HDH system, Gabrielli [24] investigated the design and operation of an HDH process coupled with PVT module. The mathematical models were established to simulate the different components of the process, and the performance of the proposed system was analyzed. It was found that a configuration with two series-connected solar modules represented the optimal trade-off in terms of water and electricity generation, and the proposed system had better performance and applicability compared to conventional solar-driven HDH units.

1.2. Goals of the study

Regarding the previous literature survey, the conclusion can be given that the dual-heated solar based HDH desalination system have drawn some attentions, and the thermodynamic performance were preliminarily investigated [25,26]. However, it was also discovered only the superiority of the water production capacity was validated, and the detailed comprehensive performance, including the thermodynamic and economic aspects, was not fully studied. Furthermore, it was focused that the coupling of PV/T and HDH can be applied to achieve water and power production at the same time. However, in order to further utilize the renewable energy, the combination of the PV/T and solar air collector, acting as the heat sources, is innovative to fully take advantages of the dual-heated configurations based on the HDH cycle, which was not concerned at all. Consequently, a novel dual-heated WPCS was built to produce water and electricity, in which PV/T was used for seawater heating and electricity generation while solar collector is applied for air heating. Comprehensive performance of the WPCS were investigated, and influence principles from the PED, solar intensity were revealed. The advantages of the proposed dual-heated WPCS are validated through the performance comparison. The research method and results provide important significance to design and further optimize the HDH desalination systems.

2. Modeling

2.1. Definition of a dual-heated WPCS

Configuration details of the dual-heated WPCS are shown in Fig. 1, which consist of the PV/T module, solar air collector, filling humidifier and dehumidifier as a heat exchanger, air-blowers and pumps. It is obvious that three different streams, including the seawater, freshwater and humid air, are existing in the desalination framework. Seawater is pumped flowing in the dehumidifier, condensing the humid air, and it is also preheated. After that, the seawater temperature is further elevated in the photovoltaic cell.

The seawater is sprayed into the packed bed humidifier, direct contacting the cold air from the dehumidifier, while the air temperature and humidity ratio rise. And then the seawater is concentrated in the humidifier and discharged from the bottom of humidifier. On the other hand, the saturated and hot air after humidification is heated in the solar collector. After that, the heated air is again cooled and condensed in the dehumidifier along with a heat and mass transfer process with the seawater. As a result, the cold air is obtained and freshwater is produced, with the airflow closed. The seawater flows into the PV/T module to be heated before entering the humidifier. In addition of the water production, the PV cell gives out electricity, which can be used to power the blowers and pumps, while the remaining power also acts as the production of the combined system.

The core heat and mass transfer processes in the humidifier, dehumidifier, solar collector and PV/T module are described in the T-i diagram in Fig. 2.

In order to complete the comprehensive investigation for the WPCS successfully, the conditions are assumed as follows:

- The WPCS operates at a steady-state condition.
- Heat dissipation to the surroundings, and kinetic and potential energy changes in the WPCS are ignored.
- Foulings of the heat and mass transfer devices are not considered.

2.2. Conservation equations

2.2.1. PV/T unit

The type of water cooling in the PVT unit is bottom cooling. The pipes are embedded into the flow channel of the seawater at the bottom of the PVT module. Regarding the photoelectric converting process, with the detailed

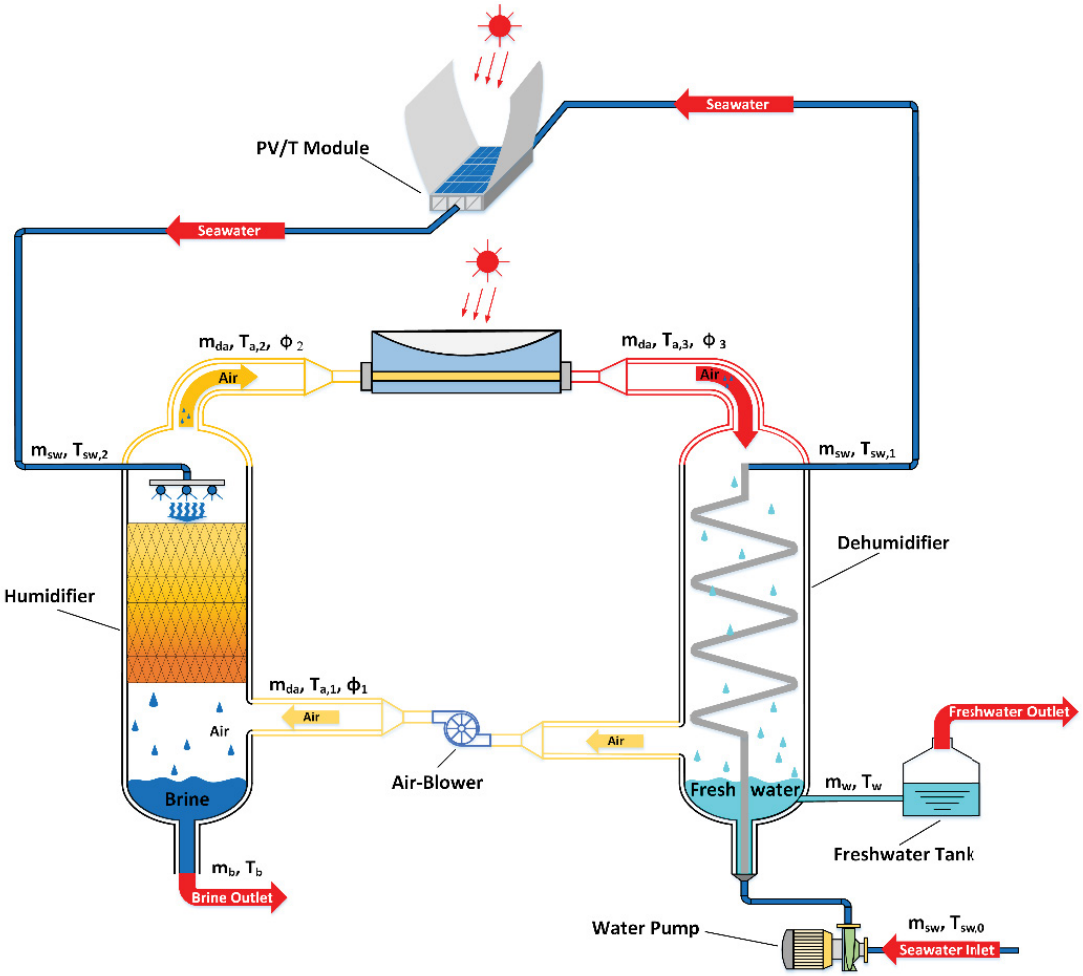

Fig. 1. Configurations of the dual-heated WPCS.

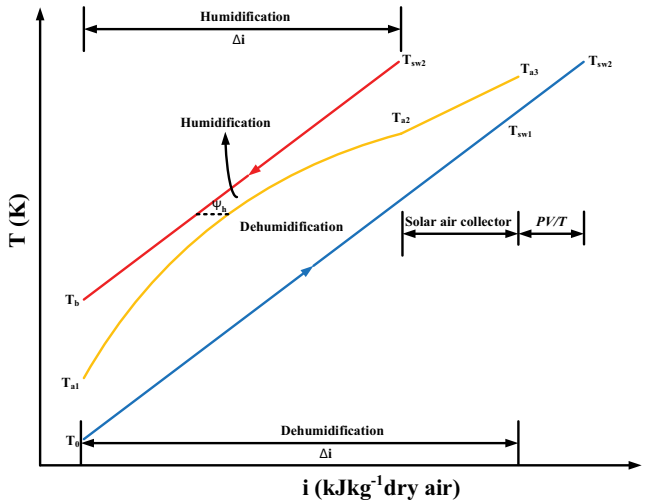

Fig. 2. T-i diagram of the thermal processes within the dual-heated WPCS.

Table 1
Structure and dimension details of the PV/T unit

Parameter	Value
c	3
I, Wm^{-2}	800
α_g	0.1
τ_g	0.9
εm_{g1}	0.88
α_c	0.9
β_c, 1/K	0.0045
T_{ref}, K	298.15
η_{ref}, %	20
δ_{g1}, m	0.004
δ_{g2}, m	0.003
δ_{g3}, m	0.004
δ_E, m	0.0001
δ_C, m	0.0003
δ_I, m	0.01
λ_{g1}, Wm^{-1}·K^{-1}	0.7
λ_{g2}, Wm^{-1}·K^{-1}	1
λ_{g3}, Wm^{-1}·K^{-1}	0.7
λ_E, Wm^{-1}·K^{-1}	0.35
λ_C, Wm^{-1}·K^{-1}	148
λ_I, Wm^{-1}·K^{-1}	0.035
$S_{PV/T}$, m^2	15
L_g, m	1.5
H_g, m	0.025

information in Table 1, the generated power in the PV cell can be calculated according to Eq. (1) [27]:

$$E_c = cI\tau_g\alpha_c\eta_c S_c \tag{1}$$

$$\eta_c = \eta_{\text{ref}}\left[1-\beta_c\left(T_c - T_{\text{ref}}\right)\right] \tag{2}$$

PV/T unit is mainly made up of a solar concentrator, PV cell and seawater channels. In the compound parabolic concentrators (CPC), solar energy is concentrated and then collected in the PV/T unit, and thus electricity is generated, with the PV cell temperature rising. According to the PV principles, the solar-electricity efficiency depends on the PV cell temperature, and the inflow seawater is pumped to remove the released heat from the PV cell. Accordingly, the temperature of the seawater through the lower covering glass is promoted. The equilibrium equations to describe the photothermal conversion can be given as follows [28]:

$$cI\alpha_g + K_{\text{cg1}}\left(T_c - T_{g1}\right) = K_{g1\text{amb}}\left(T_{g1} - T_{\text{amb}}\right) + K_{g1\text{sky}}\left(T_{g1} - T_{\text{sky}}\right) \tag{3}$$

$$Q_c = K_{\text{cg2}}\left(T_c - T_{g2}\right) + K_{\text{cg1}}\left(T_c - T_{g1}\right) + \frac{E_c}{S} \tag{4}$$

$$K_{\text{cg2}}\left(T_c - T_{g2}\right) = h_f\left(T_{g2} - T_f\right) \tag{5}$$

$$h_f\left(T_{g2} - T_f\right) = \frac{m_{\text{sw}}c_{\text{sw}}\left(T_{\text{sw},o} - T_{\text{sw},i}\right)}{S + K_{\text{famb}}\left(T_f - T_{\text{amb}}\right)} \tag{6}$$

$$Q_{\text{sw}} = m_{\text{sw}}c_{\text{sw}}\left(T_{\text{sw},o} - T_{\text{sw},i}\right) \tag{7}$$

$$\begin{cases} K_{\text{cg1}} = \dfrac{1}{\dfrac{\delta_{g1}}{2\lambda_{g1}} + \dfrac{\delta_E}{\lambda_E} + \dfrac{\delta_c}{2\lambda_c}} \\ K_{\text{cg2}} = \dfrac{1}{\dfrac{\delta_{g2}}{\lambda_{g2}} + \dfrac{\delta_E}{\lambda_E} + \dfrac{\delta_c}{2\lambda_c}} \\ K_{g1\text{amb}} = \dfrac{1}{\dfrac{\delta_{g1}}{2\lambda_{g1}} + \dfrac{1}{h_{\text{amb}}}} \\ K_{g1\text{sky}} = \sigma\varepsilon_g\dfrac{T_{g1}^4 - T_{\text{sky}}^4}{T_{g1} - T_{\text{sky}}} \\ K_{\text{famb}} = \dfrac{1}{\dfrac{1}{h_f} + \dfrac{\delta_{g3}}{\lambda_{g3}} + \dfrac{\delta_i}{\lambda_i} + \dfrac{1}{h_{\text{amb}}}} \end{cases} \tag{8}$$

The convective coefficient of the heat transferring, between the channel seawater and upper glass cover can be calculated in Eq. (9) [29]:

$$\begin{cases} h_{\text{sw}} = \text{Nu}\lambda_{\text{sw}} / D_H \\ \text{Nu} = 7.54\left(\text{Re} < 2300\right) \\ \text{Nu} = 0.023\,\text{Re}^{0.8}\,\text{Pr}^{0.4}\left(\text{Re} > 2300\right) \end{cases} \tag{9}$$

Finally, after the production is harvested as electricity and thermal energy from the PV/T module, the total efficiency can be given as:

$$\eta_{PV/T} = \frac{Q_{sw} + E_c}{cIS_{PV/T}} \tag{10}$$

2.2.2. Solar air collector

For the purpose to raise the air temperature from the humidifier, a solar collector with the structure and dimensions in Table 2, is installed in the HDH desalination configuration, and the corresponding characteristics can be calculated by the following equation in Eq. (11) [20]:

$$\begin{cases} F' = \dfrac{1}{1+\dfrac{U_L}{h_1+\dfrac{1}{\dfrac{1}{h_2}+\dfrac{1}{h_r}}}} \\ F_R = \dfrac{m_a C_p}{AU_L}\left(1-e^{-AU_L\frac{F'}{m_a C_p}}\right) \\ Q_u = m_{da}\left(i_{a_3}-i_{a_2}\right) \\ Q_u = AF_R\left(I_e - U_L\left(T_{a2}-T_0\right)\right) \\ U_L = U_e + U_t + U_b \\ T_p = T_{a2} + \dfrac{Q_u/A}{F_R U_L}\left(1-F_R\right) \end{cases} \tag{11}$$

Accordingly, after the air collector performance is simulated, the corresponding energy conversion efficiency can be concluded as:

$$\eta_{SAC} = \frac{Q_u}{IS_{SAC}} \tag{12}$$

2.2.3. Dehumidifier

Humidified and heated in the ASC, the air with a top temperature goes into the plate heat exchanger based dehumidifier, and the carried vapor is condensed and removed as the production, cooled by the seawater, with the balance equations as:

$$m_w = m_{da}\left(\omega_3 - \omega_1\right) \tag{13}$$

$$Q_d = m_{sw}\left(i_{sw,1} - i_0\right) = m_{da}\left(i_{a3} - i_{a1}\right) - m_w i_w \tag{14}$$

Table 2
Detailed information of the solar air collector

Parameter	Value
I, Wm^{-2}	800
α_g	0.1
τ_g	0.9
δ_g, m	0.004
δ_p, m	0.01
λ_g, Wm^{-1}·K^{-1}	0.7
λ_p, Wm^{-1}·K^{-1}	0.035
S_{ASC}, m^2	5

For the plate heat exchanger based dehumidifier, the dehumidification performance can be described by the general effectiveness definition as [30]:

$$\begin{cases} \varepsilon_d = \dfrac{\Delta I_t}{\Delta I_{t\max}} \\ \Delta I_{t\max} = \min\left(\Delta I_{t\max,sw}, \Delta I_{t\max,air}\right) \end{cases} \tag{15}$$

For the purpose to achieve the WPCS performance analysis, the dehumidifier heat transfer area should be obtained, considering the convective heat transfer coefficients both of the seawater and air.

Muley and Manglik [31] summarized the Nusselt number function for the compact heat exchanger, and the relevant dimensions in the current study are exhibited in Table 3.

$$\begin{aligned} \mathrm{Nu} = &\left(0.2668 - 0.006967\gamma + 7.244\times10^{-5}\gamma^2\right) \\ &\left(20.78 - 50.94\varphi + 41.16\varphi^2 - 10.15\varphi^3\right) \\ &\mathrm{Re}^{\left(0.728+0.0543\sin\left(\pi\gamma/45+3.7\right)\right)}\,\mathrm{Pr}^{1/3}\left(\mu/\mu_w\right)^{0.14} \end{aligned} \tag{16}$$

For the dry air based heat transferring, the corresponding convective heat transfer coefficient, h_d, can be given as Eq. (16). However, for the wet conditions with steam condensation, the actual coefficient, h_w, can be updated in Eq. (17) [32]:

$$h_w = h_d\left(0.164\ln\left(\mathrm{Re}\right) - 0.02\right) \tag{17}$$

Therefore, the convective coefficient of the seawater and air, the total coefficient, K, can be attained, and the dehumidifier area can be expressed in Eq. (18).

$$S_d = \frac{Q_d}{K_d \Delta T_d} \tag{18}$$

At the aspect of the flow resistance within the dehumidifier, the flow loss both for the air and seawater can be attained from the Eq. (19) [31].

$$\begin{cases} f = \left(2.917 - 0.1277\gamma + 2.016\times10^{-3}\gamma^2\right) \\ \qquad \left(5.474 - 19.02\varphi + 18.93\varphi^2 - 5.341\varphi^3\right) \\ \qquad \mathrm{Re}^{-\left(0.2+0.0577\sin\left(\pi\gamma/45+2.1\right)\right)} \\ \Delta p = 2f\dfrac{L}{D_h}\left(\rho v^2\right)\left(\mu/\mu_w\right)^{-0.17} \end{cases} \tag{19}$$

Table 3
Structure and dimension details of the dehumidifier

S_p (mm^2)	40,460
δ (mm)	0.45
b (mm)	4.3
W (mm)	60
γ (°)	60
ϕ	1.3

2.2.4. Filling humidifier

Seawater is preheated and further heated in the dehumidifier and PV/T module, and then it is injected into the filling. Hence, the air temperature and humidity, are raised, when the seawater and air contact directly, within the small filling channels in accordance with the governing equations.

$$m_{\mathrm{sw}} - m_b = m_{\mathrm{da}}\left(\omega_2 - \omega_1\right) \tag{20}$$

$$m_{\mathrm{sw}} i_{\mathrm{sw},2} - m_b i_b = m_{\mathrm{da}}\left(i_{a2} - i_{a1}\right) \tag{21}$$

During analyzing the performance of the WPCS, a new definition of effectiveness from Lienhard [33], ε_h, is applied to fix the thermodynamic parameters at the boundaries of the filling humidifier in Eq. (22).

$$\varepsilon_h = \frac{\Delta i}{\Delta i + \psi_h} \tag{22}$$

On the basis of the humidification parameters, the mass transfer coefficient, k_h and filling dimensions, D_h and H_h can be gained [34,35]:

$$m_{\mathrm{da}}\left(i_{a2} - i_{a1}\right) = k_h a_p V_h \left[\frac{\left(i_{\mathrm{sw},2s} - i_{a2}\right) - \left(i_{b,s} - i_{a1}\right)}{\log\left(\frac{i_{\mathrm{sw},2s} - i_{a2}}{i_{b,s} - i_{a1}}\right)}\right] \tag{23}$$

$$\frac{k_h a_p V_h}{m_{\mathrm{sw}} / \left(\frac{\pi}{4} D_h^2\right)} = \left(1.222 H_h + 0.367\right)\left(\frac{m_{\mathrm{sw}}}{m_{\mathrm{da}}}\right)^{(-0.66)} \tag{24}$$

2.2.5. Air-blower and pump

Power dissipation of the pumps and blowers in the WPCS is considered evaluating the comprehensive performance. The blower is used to overcome the resistance from the air channels [36], flowing through the fillings, solar air collector and plate heat exchanger based dehumidifier. As a result, the air-blower power can be expressed, with the efficiency fixed at $\eta_b = 0.8$:

$$W_{\mathrm{bl}} = \frac{m_a}{\rho_a \eta_{\mathrm{bl}}}\left(\Delta p_{\mathrm{SAC}} + \Delta p_h + \Delta p_{d,a}\right) \tag{25}$$

In order to cycle the seawater within the WPCS, the pump is also involved, and the pump power can be acquired, with the efficiency at $\eta_p = 0.8$ and spraying pressure at $p_s = 300{,}000$Pa.

$$W_{\mathrm{sp}} = \frac{m_{\mathrm{sw}}}{\rho_{\mathrm{sw}} \eta_{\mathrm{pu}}}\left(\Delta p_{\mathrm{PV}/T} + \Delta p_{d,\mathrm{sw}} + p_s\right) \tag{26}$$

2.3. Economic aspect

After the thermodynamic performance and specific structure details of the WPCS are obtained, the relevant economic investigation can be completed in accordance with the component dimensions and prices:

$$\begin{cases} C_h = V_h P_p \\ C_d = \rho_{\mathrm{d}} S_d \delta_d P_d \\ C_{\mathrm{PV}/T} = f\left(S, E, \mathrm{CRC}\right) \\ C_{\mathrm{ASC}} = f\left(S, m, T\right) \\ C_{\mathrm{bl}} = f\left(W_{\mathrm{bl}}\right) \\ C_{\mathrm{sw}} = f\left(W_{\mathrm{sw}}\right) \end{cases} \tag{27}$$

Therefore, total cost of the solar driven WPCS can be obtained based on the component cost, exhibited in Table 4. The system annual cost (AC) can be determined, in the light of the annual maintenance cost (AMC), fixed annual cost (FAC) and annual salvage value (ASV) [37], can be attained. Hence, the total annual yield (AY) and PBP can be gained to weigh the WPCS economic performance.

For the purpose to characterize the comprehensive performance of the WPCS, GOR is proposed to demonstrate the energy conversion conditions:

$$\mathrm{GOR} = \frac{m_{\mathrm{pw}} h_{\mathrm{fg}}}{Q_{\mathrm{sw}} + Q_u + W_{\mathrm{bl}} + W_p} \tag{28}$$

3. Mathematical model validation

As the core devices of the dual-heated WPCS, mathematical models for the humidifier, PV/T module and dehumidifier are validated by the published literature. Temperature curve along the non-dimensional direction under $\Psi_h = 20$ kJ·kg^{-1} is contrasted with the results from Chehayeb et al. [38] in Fig. 3 during the humidification, and the peak deviation of the seawater temperature at the outlet arises as 0.65%. For the PV/T module calculation results from Bu [39], it can be found in the Table 5 that the maximum relative errors emerges at the value of photovoltaic efficiency with a magnitude of 6.54%. For the validation of the solar collector, the comparison results between the dual-heated WPCS system and that from Chen [40] are presented in the Table 6, and it is obvious that the relative error of $T_{\mathrm{sw},2}$ is 0.146%, which is within an acceptable range in engineering practice.

Table 4
Prices of the contained components in the dual-heated WPCS

Sub-system	Components	Price
PV/T	PV cell ($)	666.67
	Cover plate ($)	111.63
	Heat transfer channels ($)	279.07
	Accessory ($)	465.12
SAC	CPC ($)	872.09
	Collector ($)	852.71
HDH	Fillings ($m^{-3})	310.08
	Titanium alloy ($kg^{-1})	40.31
	Blowers ($)	192.25
	Pumps ($)	120.93

Moreover, the dehumidification performance is verified by the published data from He [5], with a top deviation of 0.07% for the outlet air temperature. Therefore, it can be concluded that the small errors both for the humidification and dehumidification prove the model accuracy for the dual-heated WPCS.

4. Results and discussion

Comprehensive performance of the dual-heated WPCS is attained under the appointed conditions, in Table 7. PED with Ψ_h = 10 kJ·kg^{-1} is fixed, while the dehumidifier effectiveness is designated at ε_d = 0.85. Furthermore, the areas of the PV/T and solar collector are 15 and 5 m^2, respectively.

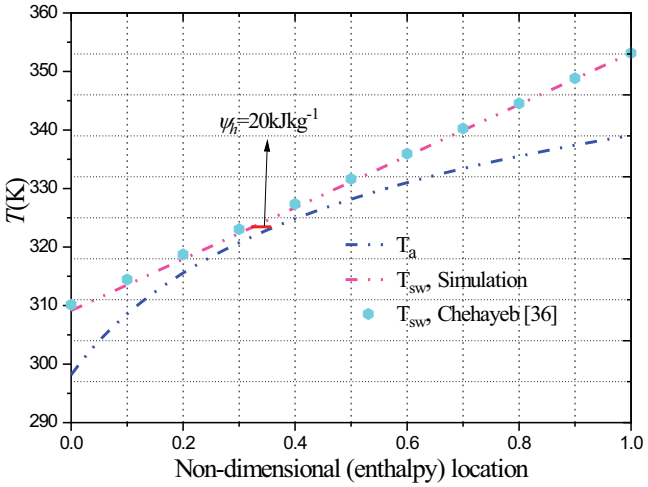

Fig. 3. Temperature profiles during humidification for the dual-heated WPCS and that from Chehayeb et al. [38].

Table 5
Validation of the PV/T module

Term	I (W/m^2)	$T_{sw,1}$ (°C)	m_{sw} (kg/s)	E_c (W/m^2)	η_c (%)
Calculation	1,000	28	0.028	406.16	12.54
Bu [39]	1,000	28	0.028	410.71	11
Relative error (%)	–	–	–	–0.56	6.54

4.1. Performance of the PV/T unit and solar air collector

In the PV/T unit within the WPCS, feed seawater is employed to remove the heat from the PV cell for raising the solar-electricity conversion efficiency, and the specific performance is shown in Fig. 4. It is validated that removing heat from the PV cell is beneficial to the total efficiency of the PV/T unit, and the corresponding top values for the heat removing and comprehensive efficiency are 17.17 kW and 59.31%, respectively. However, owing to the coupling of the PV/T and desalination system, the bottom electric power and photoelectric conversion efficiency still arises as E_c = 4.18 kW and η_c = 14.34%, because of a top temperature for the PV cell at the dehumidifier balance condition. It is also found the PV/T performance is not related to the humidifier balance condition, HCR_h = 1, due to the application of PED method [41] during designing the humidifier.

Table 6
Validation of the solar collector

Term	I (W/m^2)	$T_{sw,1}$ (°C)	m_{sw} (kg/s)	S_{ASC} (m^2)	$T_{sw,2}$ (°C)
Calculation	1,000	106.31	0.028	2.38	178
Chen [40]	1,000	106.31	0.028	2.38	177.74
Relative error (%)	–	–	–	–	0.146

Table 7
Prescribed conditions of the dual-heated WPCS

SC (g·kg^{-1})	35
Ψ_h (kJ·kg^{-1})	10
ε_d	0.85
Φ	1
$T_{sw,0}$ (K)	303.15
m_{sw} (kg·s^{-1})	0.5
a (m^2·m^{-3})	800
D_h (m)	0.4

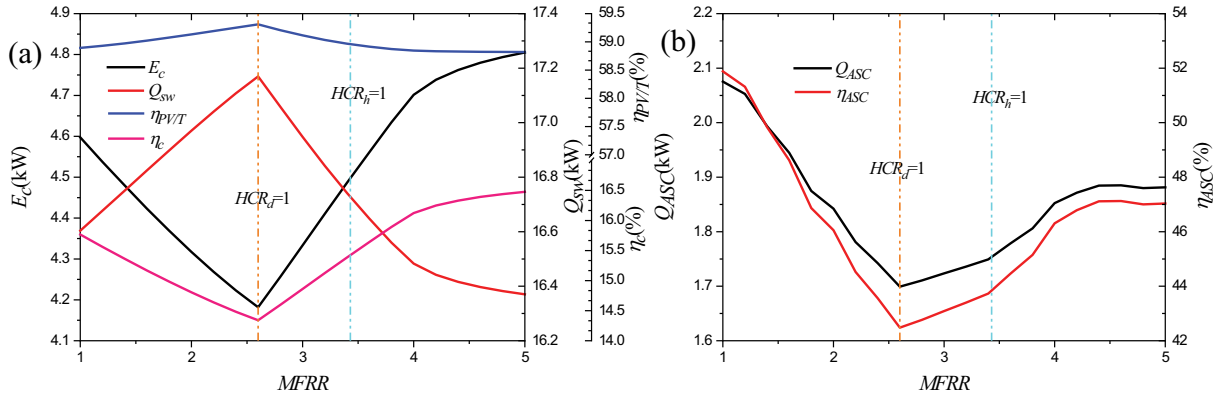

Fig. 4. Performance of the (a) PV/T and (b) solar air collector in the dual-heated WPCS at the assigned conditions.

For the solar air collector, minimum values of the heat capacity and the corresponding thermal efficiency are obtained as Q_{ASC} = 1.70kW and η_{ASC} = 42.48%, because the temperature of the collector plate is the highest at the case of HCR_d = 1.

4.2. Thermodynamic performance of the dual-heated WPCS

After modelling all the contained components, thermodynamic performance of the dual-heated WPCS is simulated and analyzed. It was demonstrated and validated that the state of dehumidification balance condition, HCR_d = 1, was especially significant for the dehumidification and desalination performance. Actually, due to the fixed dehumidification effectiveness, the denominator of the effectiveness definition in Eq.(15), which indicates the bottom value of the maximum total enthalpy difference, ΔI_t, will alternated before and after the case of HCR_d = 1, and the relevant change trends will also reversed. As a result, almost all the variables with the HDH desalination system will have a transition, when the balance condition appears [42]. Hence, it is seen in Fig. 5a the temperatures both of the seawater and air get their maximum values before and after heating in the PV/T unit and solar air collector, which represents the optimal heat transfer efficiency at the dehumidifier balance condition, and the corresponding MFRR is found at MFRR = 2.6. In response to the special PV/T performance at the balance condition, a peak seawater temperature rise, 8.52 K, is obtained, which contributes to the maximum heat capacity removing from the PV cell. For the solar air collector, the temperature elevation after the heating expands gradually from 3.63K at MFRR = 1 to 16.43 K at MFRR = 5.

Furthermore, specific performance of the dual-heated WPCS is shown in Fig. 5b. It is evident the difference of the air humidity ratio at the inlet and outlet of the humidifier reaches a top value, 0.11 kg·kg^{-1}, at the dehumidifier balance condition, and the relevant maximum water yield, m_w = 76.32 kg·h^{-1}, emerges naturally. As the GOR definition in Eq. (28), consumed power of the air-blower and pump is taken into account during evaluating the energy conversion efficiency of the dual-heated WPCS. It is distinct in Fig. 5c power consumption of the air-blower is much higher than that of the pump, with a maximum power difference with 0.74 kW at MFRR = 3. Considering the water yield, heat capacity of the seawater removed from the PV cell and total consumed power together, the comprehensive efficiency of the dual-heated WPCS is obtained with GOR = 2.55, at the dehumidifier balance condition. After simulating the WPCS performance, especially for the power generation and consumption, it can be concluded that there is surplus electricity, and the proposed system can fulfil the goal of water and power combined production for the full range of the prescribed MFRR. Taking the balance case into account, the surplus power generated in the PV is 3.35 kW, which can be applied for other occasions.

In addition, the detailed structure parameters of the filling and heat exchanger based dehumidifier are calculated and gained in Fig. 5b. At the dehumidifier balance condition, which responds to the best state of the dual-heated WPCS, the area of the dehumidifier arrives at S_d = 128.83 m^2,

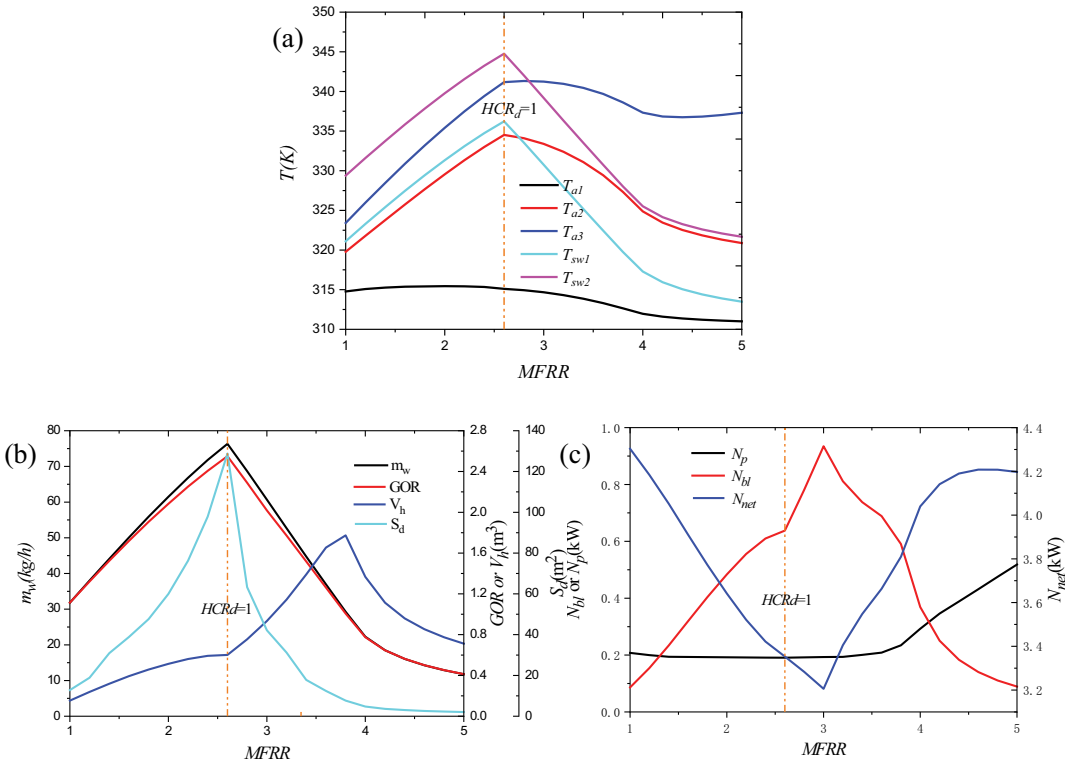

Fig. 5. Comprehensive performance of the dual-heated WPCS at the assigned conditions. (a) Temperature, (b) desalination performance and (c) power.

while the volume of the dehumidifier, V_h, is obtained as V_h = 0.60 m^3.

4.3. Economic performance of the dual-heated WPCS

After the specific characteristics of the whole dual-heated WPCS are determined, the cost of all the contained devices and system can be calculated and obtained, with the specific prices of the PV/T, solar air collector, dehumidifier material, fillings, blowers and pumps shown in Table 4. It is found the investments of the PV/T and solar air collector arrive at $2,394.38 and $852.71, respectively, while the most expensive device is the dehumidifier with a cost of $35,108.92 due to an area of 128.83 m^2, and the total cost of the dual-heated WPCS is $38,855.55 at the dehumidifier balance condition. In accordance with the economic analysis method, the specific economic aspect of the dual-heated WPCS is simulated and presented in Fig. 6.

AY and WPC obtained from produced water and electricity accommodation and PBP of the dual-heated WPCS are obtained, with the interest rate, i, working lifetime, n, electricity price, P_{ele}, and annual operation time, t_r, fixed at 12%, 10 y, 0.13 $kWh^{-1} and 2,920 h, respectively listed in Table 8. It is found the system AC exceeds the AY in the middle of the MFRR range, and the AY fluctuation of the dual-heated WPCS is very limited at all the three appointed water prices.

At the aspect of the PBP, the appearance of the longest value is discovered at the dehumidifier balance case, resulting from the component cost illustrated above, especially for the heat exchanger based dehumidifier, and the longest PBP at different water prices, P_w = 0.78, 1.55 and 3.10 $t^{-1}, are calculated as 55.28, 49.27 and 44.44 y, with the economic performance of the dual-heated WPCS in Table 8. As a result, it is impossible to recover the total cost of the dual-heated WPCS within the design working lifetime, although economic impossibility of investment return is of less importance in areas with water shortages.

4.4. Parametric analysis of the dual-heated WPCS

4.4.1. PED of the humidifier

After analyzing the comprehensive performance of the dual-heated WPCS, the parametric investigation can be fulfilled to announce the related influence law. It is stated that the PED method is applied during designing the fillings in the humidifier, and thus the PED between the seawater and air is selected to explore the potential influences on the dual-heated WPCS. It is revealed a smaller difference during humidification implies a better heat and mass transferring efficiency, which will contribute to raise the air humidity difference before and after humidification.

As a result, it can be seen in Fig. 7 fresh water condensed from the dehumidifier, m_w, is elevated from 73.41 kg·h^{-1} at Ψ_h = 15 kJ·kg^{-1} to 78.64 kg·h^{-1} at Ψ_h = 5 kJ·kg^{-1} at the case of HCR_d = 1, while the lowest net power output generated from the PV cell declines from N_{net} = 3.29 kW to N_{net} = 3.13 kW. Considering the produced water, involved thermal energy in the PV unit and collector from the solar radiation, and power expenditure together, the GOR value rises from 2.47 at Ψ_h = 15 kJ·kg^{-1} to 2.62 at Ψ_h = 5 kJ·kg^{-1} at the balance condition.

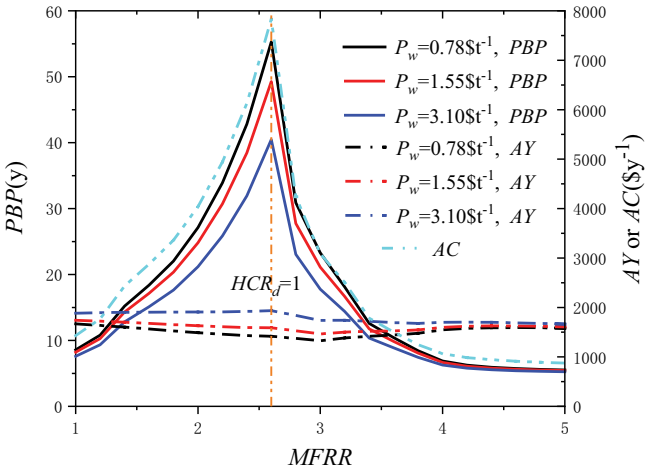

Fig. 6. Economic characteristics of the dual-heated WPCS.

Table 8
Economic characteristics of the dual-heated WPCS at the balance condition

Term	P_w (t^{-1})		
	0.78	1.55	3.10
C_t, $	38,855.55		
CRF, $	0.18		
SFF, $	0.057		
FAC, $	6,876.82		
SV, $	1,375.36		
ASV, y^{-1}	78.37		
AMC, y^{-1}	1,031.52		
AC, y^{-1}	7,829.97		
WPC, t^{-1}		15.14	
AY, y^{-1}	1,416.32	1,589.06	1,761.81
PBP, y	55.28	49.27	44.44
i, %	12		
n, y	10		
P_{ele}, kWh^{-1}	0.13		
t_r, h	2,920		

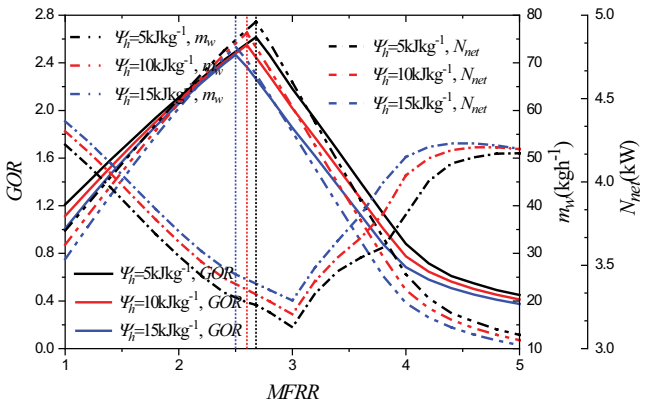

Fig. 7. Thermodynamic performance of the dual-heated WPCS with the PED during humidification.

In addition of the thermodynamic side, economic performance of the dual-heated WPCS is also simulated, and the corresponding results at different PED are listed and compared in Table 9.

It is obtained that the elevation amplitude of the annual and total cost for the dual-heated WPCS is about 3.12%, when the PED varies from 15 to 5 kJ·kg^{-1}, at the balance condition. In Fig. 7, it is found that the PED ascent will result in the rising of the net power output from the PV cell, which gives the reasons why the annual yield increases instead, and PBP have a reverse trend in response to the change of the PED.

4.4.2. Solar intensity

There are two solar involved devices in the current proposed system, including the PV unit to provide electricity as well as heating the seawater and raise the air temperature after humidification. Hence, the alternation of the solar radiation will change the energy source of the system, and the corresponding performance of the dual-heated WPCS will differ. Based on the fixed structure of the PV/T and solar air collector, temperatures both of the heated seawater and air will rise corresponding to the elevation of the solar intensity, and the relevant humidity ratio difference during humidification expands from 0.07 kg·kg^{-1} at 600 Wm^{-2} to 0.15 kg·kg^{-1} at 1,000 Wm^{-2} for each balance condition. Accordingly, the water production increases with a highest magnitude of 59.06% from 58.26 to 92.67 kg·h^{-1}, with the related net power from 2.34 to 4.23 kW, shown in Fig. 8.

However, the total thermal energy into the dual-heated WPCS from the PV/T and solar air collector also rises from 13.95 to 23.81 kW, and the final gained out ratio, GOR, decrease to 2.49 for a higher solar intensity with I = 1,000 Wm^{-2} compared to the value of 2.57 at I = 600 Wm^{-2}. The change of the solar intensity will also influence the economic performance of the dual-heated WPCS shown in Table 10. It can be found the positive effects to advance the annual yield attributed to the solar intensity elevation appears, and the shortest PBP can be reduced to 37.49 y at p_w = 1.55 \$t^{-1}, when the solar intensity stays at I = 1,000 Wm^{-2}.

5. Performance comparison to the single heated HDH desalination system

In the current dual-heated WPCS, PV/T and solar collector are applied to heat the streams of seawater and air, respectively, and the relevant comprehensive performance are simulated and presented previously. In order to validate the advantages for the aforementioned frame, performance comparison among the dual-heated WPCS and single heated HDH desalination system are achieved, exhibited in Table 11.

In order to gain the rationality of such comparison, the equivalent temperatures for the seawater or air are determined by choosing the areas of the solar air collector and PV/T. Obviously, the water-heated HDH desalination system has a relatively higher water production and lower GOR, while the situation of the air-heated type has the reverse trend. It can be summarized the features of the single heated HDH desalination systems are neutralized by proposing the current dual-heated WPCS, which also has the most superior performance in the economic aspect at the condition of P_w = 1.55 \$t^{-1}.

6. Conclusions

In this paper, PV/T module and solar air collector are both applied to act as heat sources to raise the seawater and air temperatures. Comprehensive performance of the dual-heated WPCS is simulated and analyzed, and the influences from the PED and solar intensity are studied. After

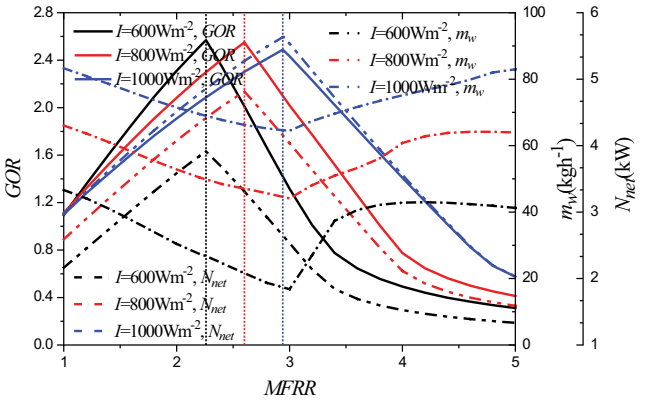

Fig. 8. Performance of the dual-heated WPCS with the solar intensity.

Table 9
Performance of the dual-heated WPCS at different PED

Ψ_h (kJ·kg^{-1})	P_w (\$t^{-1})	C_t (\$)	AC (\$y^{-1})	AY (\$y^{-1})	PBP (y)
	0.78			1,387.71	56.74
5	1.55	39,073	7,873.79	1,565.72	50.29
	3.10			1,743.73	45.15
	0.78			1,416.32	55.28
10	1.55	38,855.55	7,829.97	1,589.06	49.27
	3.10			1,761.81	44.44
	0.78			1,443.85	52.88
15	1.55	37,889.5	7,635.29	1,610.01	47.42
	3.10			1,776.17	42.99

Table 10
Economic performance of the dual-heated WPCS at different solar intensity

I (Wm^{-2})	P_w (\$t^{-1})	C_t (\$)	AC (\$y^{-1})	AY (\$y^{-1})	PBP (y)
	0.78			999.09	73.86
600	1.55	36,617.1	7,378.88	1,130.97	65.24
	3.10			1,262.86	58.43
	0.78			1,416.32	55.28
800	1.55	38,855.55	7,829.97	1,589.06	49.27
	3.10			1,761.81	44.44
	0.78			1,778.69	46.33
1,000	1.55	40,895.8	8,241.12	1,988.45	41.44
	3.10			2,198.22	37.49

Table 11
Performance comparison to the single heated HDH desalination system

Frame	$S_{PV/T}$ (m²)	S_{ASC} (m²)	T_{sw2} (K)	T_{a3} (K)	m_w (kg·h⁻¹)	GOR	C_t ($)	PBP (y)
Dual-heated	15	5	344.75	341.17	76.32	2.55	38,855.55	49.27
	10		328.49		39.39	2.02	36,472.64	102.25
Water-heated	15		336.71		55.59	2.02	40,661.29	59.72
	20		343.59		68.59	1.98	43,948.62	47.72
		30	328.56	332.16	39.90	2.48	24,801.42	276.71
Air-heated		40	330.43	334.38	44.58	2.68	27,049.72	270.09
		50	336.46	341.44	59.17	3.05	29,624.3	222.86

analyzing and presenting the research results, the following conclusions are given out:

- The combined applications of the PV/T module and solar air collector in an HDH desalination system is profitable to balance the water yield and GOR, compared to the general single heated systems, and the advantages is validated through performance comparison.
- At the appointed conditions, the top water yield and GOR, arrive at 76.32 kg·h⁻¹ and 2.55, at the case of HCR_d = 1, and there is surplus generated power, 3.35 kW, for other occasion demands. Furthermore, the total cost, annual cost and water production cost of the dual-heated WPCS are attained as 38,855.55 $, 7,829.97 $y⁻¹ and 15.14 $t⁻¹ at the dehumidifier balance condition, and the longest PBPs are calculated as 55.28, 49.27 and 44.44 y at the water prices of 0.78, 1.55 and 3.10 $t⁻¹, which indicates the impossibility of recovering the investment of the cogeneration system, although economic impossibility of investment return is of less importance in areas with water shortages.
- The water yield, m_w, and GOR are elevated from 73.41 kg·h⁻¹ and 2.47 at Ψ_h = 15 kJ·kg⁻¹ to 78.64 kg·h⁻¹ and 2.62 at Ψ_h = 5 kJ·kg⁻¹ in the balance case, and the corresponding total and annual cost of the cogeneration system is raised with an amplitude of about 3.12%.
- In response to the change of the solar intensity, the highest water production rises from 58.26 kg·h⁻¹ at 600 Wm⁻² to 92.67 kg·h⁻¹ at 1,000 Wm⁻², while the value of GOR, decreases to 2.49. Furthermore, the positive effects to advance the annual yield attributing to the solar intensity elevation result in the reduction of the PBP.

Acknowledgements

The authors acknowledge the financial support provided by Natural Science Fund Project in Jiangsu Province (Grant No. BK20201294) and the Fundamental Research Funds for the Central Universities, NO. NS2022026.

Symbols

a	—	Specific area, m²·m⁻³
b	—	Dehumidifier channel height, m
c	—	Concentration ratio
C	—	Cost, $
D	—	Diameter of the filling, m
E	—	Electric power, kW
h	—	Convective heat transfer coefficient, Wm⁻²·K⁻¹
H	—	Height, m
h_{fg}	—	Latent heat, kJ·kg⁻¹
i	—	Enthalpy, kJ·kg⁻¹
I	—	Solar intensity, Wm⁻²
I_t	—	Total enthalpy, kW
k	—	Mass transfer coefficient, kg·m⁻²·s⁻¹
K	—	Total heat transfer coefficient, Wm⁻²·K⁻¹
m	—	Mass flow rate, kg·s⁻¹
N	—	Power, kW
Nu	—	Nusselt number
p	—	Pressure, MPa
P	—	Price, $t⁻¹
P_r	—	Prandtl number
Q	—	Heat load, kW
Re	—	Reynolds number
S	—	Area, m²
SC	—	Seawater concentration, g·kg⁻¹
SV	—	Salvage value, $
T	—	Temperature, K
v	—	Velocity, m·s⁻¹
V	—	Volume, m³
W	—	Channel width, m

Greek

α	—	Absorptivity
β	—	Attenuation coefficient
γ	—	Plate chevron angle, °
δ	—	Thickness, mm
σ	—	Boltzmann constant
ρ	—	Density, kg·m⁻³
μ	—	Dynamic viscosity, kg·m⁻¹·s⁻¹
ε	—	Effectiveness
ε_m	—	Emissivity
τ	—	Transmissivity
ϕ	—	Relative humidity
Ψ	—	Pinch enthalpy difference, kJ·kg⁻¹
η	—	Efficiency
λ	—	Thermal conductivity, Wm⁻¹·K⁻¹
ω	—	Humidity ratio (kg·kg⁻¹, kg water vapor/kg dry air)

Subscripts

a	—	Air
amb	—	Ambient
b	—	Brine

bl — Blower
c — Cell
d — Dehumidifier
da — Dry air
f — Fluid
g — Glass
h — Humidifier
i — Inlet
I — Insulation
m — Maximum
o — Outlet
p — Pump
r — Running
R — Recuperator
s — Saturation
sw — Seawater
t — Total
w — Water

References

[1] M. Ziyaei, M. Jalili, A. Chitsaz, M.A. Nazari, Dynamic simulation and life cycle cost analysis of a MSF desalination system driven by solar parabolic trough collectors using TRNSYS software: a comparative study in different world regions, Energy Convers. Manage., 243 (2021) 114412, doi: 10.1016/j.enconman.2021.114412.

[2] Z.H. Chang, H.F. Zheng, Y.J. Yang, Y.H. Su, Z.C. Duan, Experimental investigation of a novel multi-effect solar desalination system based on humidification–dehumidification process, Renewable Energy, 69 (2014) 253–259.

[3] M.A. Farahat, H.E.S. Fath, I.I. El-Sharkawy, S. Ookawara, M. Ahmed, Energy/exergy analysis of solar driven mechanical vapor compression desalination system with nano-filtration pretreatment, Desalination, 509 (2021) 115078, doi: 10.1016/j.desal.2021.115078.

[4] H.F. Zheng, Solar Desalination Principle and Technology, Chemical and Industry Press, Beijing, 2012.

[5] W.F. He, Y. Lu, H.H. An, X. Zhou, P.F. Su, D. Han, Parametric analysis of humidification–dehumidification desalination driven by photovoltaic/thermal (PV/T) system, Energy Convers. Manage., 259 (2022) 115520, doi: 10.1016/j.enconman.2022.115520.

[6] E. El-Said, M. Omara, M. Dahab, G. Abdelaziz, Solar desalination unit coupled with a novel humidifier, Renewable Energy, 180 (2021) 297–312.

[7] E.M.S. El-Said, M.A. Dahab, M.A. Omara, G.B. Abdelaziz, Humidification-dehumidification solar desalination system using porous activated carbon tubes as a humidifier, Renewable Energy, 187 (2022) 657–670.

[8] W.F. He, D. Han, L.N. Xu, C. Yue, W.H. Pu, Performance investigation of a novel water–power cogeneration plant (WPCP) based on humidification–dehumidification (HDH) method, Energy Convers. Manage., 110 (2016) 184–191.

[9] G. Prakash Narayan, M.H. Sharqawy, J.H. Lienhard V, S.M. Zubair, Thermodynamic analysis of humidification–dehumidification desalination cycles, Desal. Water Treat., 16 (2010) 339–353.

[10] F.A. Al-Sulaiman, G. Prakash Narayan, J.H. Lienhard V, Exergy analysis of a high-temperature-steam-driven, varied-pressure, humidification–dehumidification system coupled with reverse osmosis, Appl. Energy, 103 (2013) 552–561.

[11] K.H. Mistry, J.H. Lienhard V, S.M. Zubair, Effect of entropy generation on the performance of humidification–dehumidification desalination cycles, Int. J. Therm. Sci., 49 (2010) 1837–1847.

[12] K.H. Mistry, Second Law Analysis and Optimization of Humidification–Dehumidification Desalination Cycles, Master's Thesis, University of California, Los Angeles, 2008.

[13] A.S.A. Mohamed, M. Salem Ahmed, A.G. Shahdy, Theoretical and experimental study of a seawater desalination system based on humidification–dehumidification technique, Renewable Energy, 152 (2020) 823–834.

[14] M.H. Elbassoussi, M.A. Antar, S.M. Zubair, Hybridization of a triple-effect absorption heat pump with a humidification–dehumidification desalination unit: thermodynamic and economic investigation, Energy Convers. Manage., 233 (2021) 113879, doi: 10.1016/j.enconman.2021.113879.

[15] D.U. Lawal, N.A.A. Qasem, Humidification-dehumidification desalination systems driven by thermal-based renewable and low-grade energy sources: a critical review, Renewable Sustainable Energy Rev., 125 (2020) 109817, doi: 10.1016/j.rser.2020.109817.

[16] M.H. Hamed, A.E. Kabeel, Z.M. Omara, S.W. Sharshir, Mathematical and experimental investigation of a solar humidification–dehumidification desalination unit, Desalination, 358 (2015) 9–17.

[17] D. Saldivia, R. Barraza, D. Estay, P. Valdivia, M. Reyes, J. García, Experimental test and sensitivity analysis of performance parameters of a solar humidification–dehumidification system, Desal. Water Treat., 228 (2021) 21–35.

[18] T. Dave, V. Ahuja, S. Krishnan, Economic analysis and experimental investigation of a direct absorption solar humidification–dehumidification system for decentralized water production, Sustainable Energy Technol. Assess., 46 (2021) 101306, doi: 10.1016/j.seta.2021.101306.

[19] R. Simonetti, L. Molinaroli, G. Manzolini, Non-Dimensional Analysis of a Humidification–Dehumidification System Driven by PV/T Collectors for Desalinate Water Production, IEA SHC International Conference on Solar Heating and Cooling for Buildings and Industry, Santiago, Chile, 2019.

[20] F.A. Al-Sulaiman, M. Ifras Zubair, M. Atif, P. Gandhidasan, S.A. Al-Dini, M.A. Antar, Humidification–dehumidification desalination system using parabolic trough solar air collector, Appl. Therm. Eng., 75 (2015) 809–816.

[21] S.M. Negharchi, A. Najafi, A.A. Nejad, N. Ghadimi, Determination of the optimal model for solar humidification–dehumidification desalination cycle with extraction and injection, Desalination, 506 (2021) 114984, doi: 10.1016/j.desal.2021.114984.

[22] A. Giwa, H. Fath, S.W. Hasan, Humidification–dehumidification desalination process driven by photovoltaic thermal energy recovery (PV-HDH) for small-scale sustainable water and power production, Desalination, 377 (2016) 163–171.

[23] C. Yıldırım, İ. Solmuş, A parametric study on a humidification–dehumidification (HDH) desalination unit powered by solar air and water heaters, Energy Convers. Manage., 86 (2014) 568–575.

[24] P. Gabrielli, M. Gazzani, N. Novati, L. Sutter, R. Simonetti, L. Molinaroli, G. Manzolini, M. Mazzotti, Combined water desalination and electricity generation through a humidification–dehumidification process integrated with photovoltaic-thermal modules: design, performance analysis and techno-economic assessment, Energy Convers. Manage., 1 (2019) 100004, doi: 10.1016/j.ecmx.2019.100004.

[25] S.H. Soomro, R. Santosh, C.-U. Bak, W.-S. Kim, Y.-D. Kim. Humidification-dehumidification desalination system powered by simultaneous air-water solar heater, Sustainability, 13 (2021) 13491, doi: 10.3390/su132313491.

[26] E.Z. Mahdizade, M. Ameri, Thermodynamic investigation of a semi-open air, humidification–dehumidification desalination system using air and water heaters, Desalination, 428 (2018) 182–198.

[27] E. Skoplaki, J.A. Palyvos, On the temperature dependence of photovoltaic module electrical performance: a review of efficiency/power correlations, Sol. Energy, 83 (2009) 614–624.

[28] X.L. Zhang, X. Chen, B.H. Wang, J. Song, Performance analysis of seawater desalination system co-driven by photoelectricity & optothermal, Elec. Pow. Sci. Eng., 35 (2019) 51–56.

[29] R.V. Dunkle, Solar Water Distillation the Roof Type Still and a Multiple Effect Diffusion, International Developments in Heat Transfer, University of Colorado, 1961, p. 895.

[30] G. Prakash Narayan, K.H. Mistry, M.H. Sharqawy, S.M. Zubair, J.H. Lienhard, Energy effectiveness of simultaneous heat and mass exchange devices, Front. Heat Mass Tranfer, 023001 (2010) 1–13.
[31] A. Muley, R.M. Manglik, Experimental study of turbulent flow heat transfer and pressure drop in a plate heat exchanger with chevron plates, J. Heat Transfer, 121 (1999) 110–117.
[32] M. Sievers, J.H. Lienhard V, Design of flat-plate dehumidifiers for humidification–dehumidification desalination systems, Heat Transfer Eng., 34 (2013) 543–561.
[33] R.K. McGovern, G.P. Thiel, G. Prakash Narayan, S.M. Zubair, J.H. Lienhard V, Performance limits of zero and single extraction humidification–dehumidification desalination systems, Appl. Energy, 102 (2013) 1081–1090.
[34] M. Mehrgoo, M. Amidpour, Constructal design and optimization of a direct contact humidification–dehumidification desalination unit, Desalination, 293 (2012) 69–77.
[35] N. Niroomand, M. Zamen, M. Amidpour, Theoretical investigation of using a direct contact dehumidifier in humidification–dehumidification desalination unit based on an open air cycle, Desal. Water Treat., 54 (2015) 305–315.
[36] P. Gandhidasan, Prediction of pressure drop in a packed bed dehumidifier operating with liquid desiccant, Appl. Therm. Eng., 22 (2002) 1117–1127.
[37] E. Deniz, S. Çınar, Energy, exergy, economic and environmental (4E) analysis of a solar desalination system with humidification–dehumidification, Energy Convers. Manage., 126 (2016) 12–19.
[38] K.M. Chehayeb, G. Prakash Narayan, S.M. Zubair, J.H. Lienhard V, Thermodynamic balancing of a fixed-size two-stage humidification–dehumidification desalination system, Desalination, 369 (2015) 125–139.
[39] Y.G. Bu, Thermodynamic Study on Desalination System of Low Concentration Photovoltaic/Thermal Collector, North China Electric Power University, 2018.
[40] X. Chen, Performance and Analysis of Distillation Desalination Plant Based on PV/T, North China Electric Power University, 2018.
[41] G. Prakash Narayan, K.M. Chehayeb, R.K. McGovern, G.P. Thiel, S.M. Zubair, J.H. Lienhard V, Thermodynamic balancing of the humidification–dehumidification desalination system by mass extraction and injection, Int. J. Heat Mass Transfer, 57 (2013) 756–770.
[42] Y. Zhang, C.G. Zhu, H. Zhang, W.D. Zheng, S.J. You, Y.H. Zhen, Experimental study of a humidification–dehumidification desalination system with heat pump unit, Desalination, 442 (2018) 108–117.